Earthward flowing plasmoid: Structure and its related ionospheric signature

Q.-G. Zong,[1,2] S. Y. Fu,[3] D. N. Baker,[4] M. L. Goldstein,[5] P. Song,[1] J. A. Slavin,[5] T. A. Fritz,[6] J. B. Cao,[2] O. Amm,[7] H. Frey,[8] A. Korth,[9] P. W. Daly,[9] H. Reme,[10] and A. Pedersen[11]

Received 6 October 2006; revised 3 January 2007; accepted 17 January 2007; published 7 July 2007.

[1] An earthward moving plasmoid has been observed on 28 October 2002 by the Cluster spacecraft with simultaneous auroral viewing by the IMAGE satellite. This offers the opportunity to ascertain the optical and the evolutional signatures in the ionosphere of the earthward moving plasmoid. The ionospheric signatures observed in this paper are not substorm-related. Both the ground-based measurements and IMAGE satellite auroral observations show the ionospheric signatures moving to lower latitudes, when the earthward moving plasmoid is observed by the Cluster spacecraft. The intensity of the current in the center of the plasmoid is found to be weaker than that in the adjacent region. Also, the directions of the current in the central part of the plasmoid, different from the background cross-tail current, are more field-aligned. Those facts are consistent with the tail current closes through the substorm-like current wedge, since the cross-tail current is blocked by the plasmoid. On the other hand, the current in the earthward plasmoid may close through the interhemisphere. In this paper we demonstrate that the magnetic structures, plasmoids and flux ropes, will transport flux and energy from the distant tail to the Earth.

Citation: Zong, Q.-G., et al. (2007), Earthward flowing plasmoid: Structure and its related ionospheric signature, *J. Geophys. Res.*, *112*, A07203, doi:10.1029/2006JA012112.

1. Introduction

[2] Plasmoids/flux ropes are an important feature of various kinds of eruptive processes in astrophysical plasmas, notably during the occurrence of magnetospheric substorms and solar coronal mass ejections (CMEs). Outstanding questions about plasmoids concern their inner magnetic structure and topology, the nature of their plasmas, and their temporal and spatial evolution following release [*Baker et al.*, 2002; *Slavin et al.*, 2003a; *Deng et al.*, 2004; *Zong et al.*, 2004]. Recently, flux ropes in the tail have been further referred to as "BBF" flux ropes (earthward flux rope with a bursty bulk flow) and "plasmoid" flux ropes (tailward flux rope) [*Slavin et al.*, 2003a]. The "BBF" flux ropes are associated with $\mp$ quasi-sinusoidal ΔB_z perturbations and earthward plasma flow, whereas the "plasmoid" flux ropes are associated with $\pm\Delta B_z$ perturbations and tailward plasma flow.

[3] The earthward moving magnetic structures like plasmoids [*Zong et al.*, 2004] and BBFs [*Nakamura et al.*, 2001] have been observed; however, the evolution and interaction with the inner magnetosphere are not understood. It is essential to study the evolution of the earthward plasmoid on its way to the near-Earth region; is the earthmoving plasmoid losing its energy by interacting with ambient plasma/field? Is the earthmoving plasmoid closure with the ionosphere or with the interplanetary space? This paper will emphasize the magnetic connectivity of plasmoids to the rest of the tail and the evolution of their internal plasma populations. The properties of this plasmoid and its related auroral and ground-based signatures are addressed.

2. Plasmoid Structure

[4] As initially reported by *Zong et al.* [2004], on 28 October 2002, the Cluster spacecraft were travelling in the tail plasma sheet at GSE (−11, 11.8, 2.4) R_E in the northern part of the tail. Figure 1 gives a summary of the measurements obtained by different instruments on board Cluster between 1930 and 2000 UT on 28 October 2002.

[1]Center for Atmospheric Research, University of Massachusetts Lowell, Lowell, Massachusetts, USA.
[2]State Key Laboratory for Space Weather, Chinese Academy of Sciences, Beijing, China.
[3]Peking University, Beijing, China.
[4]Laboratory for Atmospheric and Space Physics, University of Colorado, Boulder, Colorado, USA.
[5]NASA Goddard Space Flight Center, Greenbelt, Maryland, USA.
[6]Center For Space Physics, Boston University, Boston, Massachusetts, USA.
[7]Finnish Meteorological Institute, Helsinki, Finland.
[8]Space Science Laboratory, University of California, Berkeley, California, USA.
[9]MPS, Katlenburg-Lindau, Germany.
[10]Centre d'Etude Spatiale des Rayonnements, Toulouse, France.
[11]Department of Physics, University of Oslo, Oslo, Norway.

Copyright 2007 by the American Geophysical Union.
0148-0227/07/2006JA012112

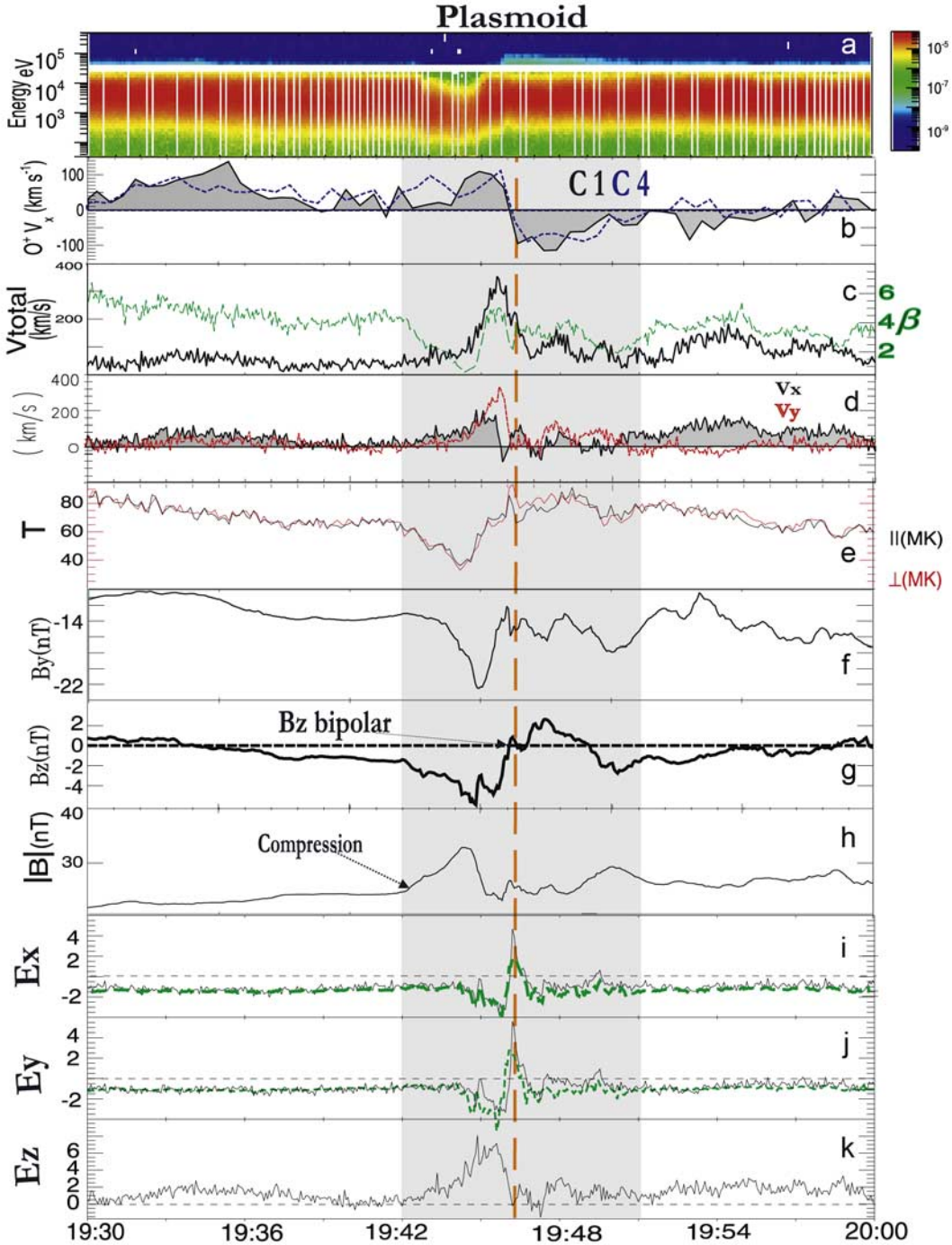

Figure 1. (a) An overview of plasma (PEACE) and energetic (RAPID) electron spectrum during the plasmoid [*Zong et al.*, 2004] together with (b) the single charged oxygen Vx, (c) plasma β, (d) plasma ion total velocity, (e) parallel and perpendicular velocity and temperature obtained by CIS instrument. Also shown are the magnetic field (f) B_z, (g) B_z, and (h) B_t and electric field (i) E_x, (j) E_y, and (k) E_z components obtained by EFW (green) and $-$V X B (black). The first shaded area is the central part of the plasmoid. The dashed orange line marks the reflection point of the plasmoid where Bz changes sign.

[5] Figure 1 shows plasma electron (PEACE) [*Johnstone et al.*, 1997] and energetic electron (RAPID) [*Wilken et al.*, 2001] spectra during the plasmoid [*Zong et al.*, 2004]. Plasma β, plasma ion parallel, and perpendicular velocity and temperature are also shown. The magnetic field B_y, B_z, and B_t are given in Figure 1f, 1g, and 1h. Figures 1i, 1j, and 1k show an intercomparison between the electric field components measured by the EFW instrument (double probe) [*Gustafsson et al.*, 2001] and the $\mathbf{E} = -\mathbf{V} \times \mathbf{B}$, where $\mathbf{V}$ is the plasma ion velocity from CIS [*Reme et al.*, 1997] and $\mathbf{B}$ is the magnetic field vector from FGM [*Balogh et al.*, 1997]. The large-amplitude bipolar electric fields E_x and E_y (between 1944 and 1948 UT) observed by EFW instrument are reproduced well by $E = -V \times B$.

[6] In the leading edge of the plasmoid (1942 to 1944 UT), the magnitude of the magnetic field increased significantly. This increase is not a betatron acceleration because both plasma ion temperature and β decreased. It is interesting to point out the single charged oxygen ions are obvious different than hydrogen ions. The Vx component of the oxygen changes sign at 1946 UT (the inflection point where Bz changes its sign). The flow direction is first earthward and after 1946 tailward. The different behavior of oxygen ion imply that the single charged oxygen ions are freshly resupplied from polar ionosphere, whereas the hydrogen ions are preexisting [*Zong et al.*, 1997, 1998].

[7] Figure 2 presents the evolution of the total current density $\mathbf{J}$ (Figure 2c) that is calculated by the linear interpolation approach for the time period of interest. The maximum current reaches $\sim$30 nA/m^2. Figure 2d shows the ratio of $\nabla \cdot \mathbf{B}/|\nabla \times \mathbf{B}|$ which has been regarded as the estimation of the relative error $\delta|\mathbf{J}|/J$ [*Robert et al.*, 1998]. It is seen that the relative error is less than ± 0.5 (meaning that $\delta|\mathbf{J}|/J < 50\%$). This indicates that in the center of the plasmoid the relative error is sufficiently small so that the curlometer technique is valid.

[8] The angles between the current and the magnetic field vector are given in Figure 2b. The current is defined as a field-aligned current if the angle is between 0° and 30° or between 150° and 180° and cross tail current if the angle is between 75° and 105° (90° ± 15°). As can be seen before the plasmoid arrival, the current in the tail plasma sheet can be considered to a great extent as being the cross-tail current. However, the current in the central part of the plasmoid turned to a direction varying between the background cross-tail direction and the anti-field-aligned direction. Only in a small region close to the plasmoid center, the current was in anti-field-aligned direction. If the current is parallel or antiparallel to the magnetic field, then the structure is quasi-force-free ($J \times B = 0$), i.e., the observed plasmoid consists of non-force-free and quasi-force-free parts (see also Figure 2f). The current in the plasmoid can then either close through the auroral ionosphere [*Kivelson et al.*, 1996] or through the solar wind-magnetosheath if the flux rope is long enough [*Hesse et al.*, 1996].

[9] The electromechanical energy conversion term in Poynting's equation ($\mathbf{J} \cdot \mathbf{E}$) is plotted in Figure 2a. We follow electrical engineering in using the terms "dynamo" ($\mathbf{J} \cdot \mathbf{E} < 0$) and "load" ($\mathbf{J} \cdot \mathbf{E} > 0$) as a conceptual heuristic [e.g., *Paschmann et al.* 1979].

[10] As the plasmoid moves toward the Earth, the plasma has to slow down, and the plasmoid becomes a "dynamo" $\mathbf{J} \cdot \mathbf{E} < 0$. The plasmoid will release energy to the ambient region. As we can see from Figure 2a, the earthward moving plasmoid is a generator. However, in the plasmoid core region where the field has a local maximum, $\mathbf{J} \cdot \mathbf{E}$ is positive because of significant positive Ex and Ey for 20 s (the scale size is estimated as 1400 km). During this interval the plasmoid behaves as being a "Load," meaning that the ambient electromagnetic energy is partly being converted into mechanical energy in the plasmoid.

[11] Furthermore, the evaluation of the total pressure which is determined by the plasma pressure (nkT) plus the magnetic pressure ($B^2/2\mu$) is shown in Figure 2e and the $\mathbf{J} \times \mathbf{B}$ force is given in Figure 2f. As can be seen, the plasmoid is in total pressure balance; however, the $\mathbf{J} \times \mathbf{B}$ force is not balanced. This indicates the movement of the plasmoid is driven by the $\mathbf{J} \times \mathbf{B}$ force. There is a bump around 1945 UT in the total pressure. This pressure enhancement seems to be caused by the minimum B_y-field (core field) [*Ieda et al.*, 1998]. Interestingly, the center of this total pressure enhancement differs from the plasmoid center at 1946 UT determined by J × B force, indicating the plasmoid having twisted geometry [e.g. *Zong et al.* 1997].

[12] The Cluster tetrahedron in GSE X-Z plane is inserted into Figure 2. Spacecraft 1 and 4 are tailward of spacecraft 2 and 3 and spacecraft 3 and 4 are closer to the $Z = 0$ plane.

3. Signatures in the Ionospheres

[13] The plasmoid characterized by the bipolar signature in B_z lasting from 1942 to 1952 UT raises some interesting questions regarding the evolution of earthward moving plasmoids in the tail plasma sheet. As earthward moving plasmoids push up against the geomagnetic field, they will probably dissipate quickly because the orientation of their magnetic field is favorable for reconnection with the geomagnetic closed field lines in the near Earth as suggested by *Slavin et al.* [2003a, 2003b] and *Zong et al.* [2004].

[14] IMAGE-FUV and Polar UVI images for 1930 to 2000 UT on 28 October 2002 support this scenario. Figure 3 and 4 shows a representative selection of images that reveal the main auroral response. The Cluster positions are mapped onto the MLT-MLAT plane with ACE solar wind data as input for the Tsyganenko-96 model in geomagnetic coordinates. As we can see, the Cluster footprints at about 70° latitude and 2000 MLT are marked by the triangle. At 1941 UT one can see a brightening close to the Cluster position, and at 1945 UT it is right under Cluster. At 1947 UT it is equatorward of Cluster.

[15] It is quite amazing that the auroral brightening occurred at 1941 UT right at the estimated Cluster position as observed by IMAGE. This is the time when the plasmoid onset occurred based on the overall Cluster particle and field data. Moreover, both the IMAGE and Polar data show the auroral forms moving to lower latitudes over the next several minutes, which coincides with the time frame during which Cluster observes the earthward moving plasmoid. Such plasmoid motion should correspond to equatorward auroral motion.

[16] As shown in Figure 3, between 1941 and 1947 UT, the aurora located in the midnight-to-dusk sector around 70° invariant latitude (Northern Hemisphere) greatly intensified. The auroral brightening are also observed in the Southern

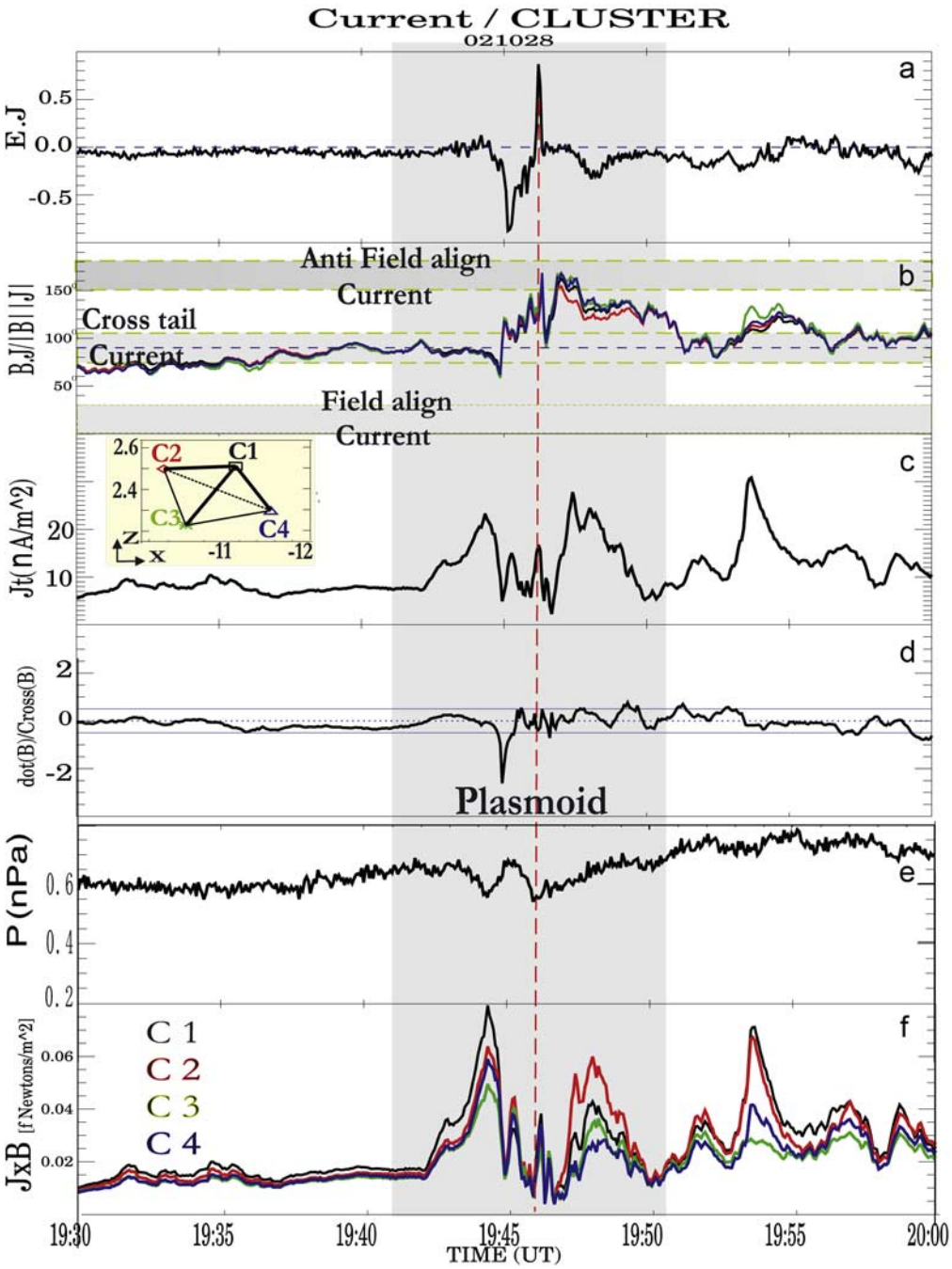

Figure 2. (a) Evaluation of the electromechanical energy conversion $E \cdot J$ where (b) the E is derived from VXB and the angle between the current and the magnetic field vector from 1930 to 2000 UT. The (c) total current density (in nA/m^2, in nA) and (d) its relative error and the (e) total pressure and (f) $J \times B$ force are also shown.

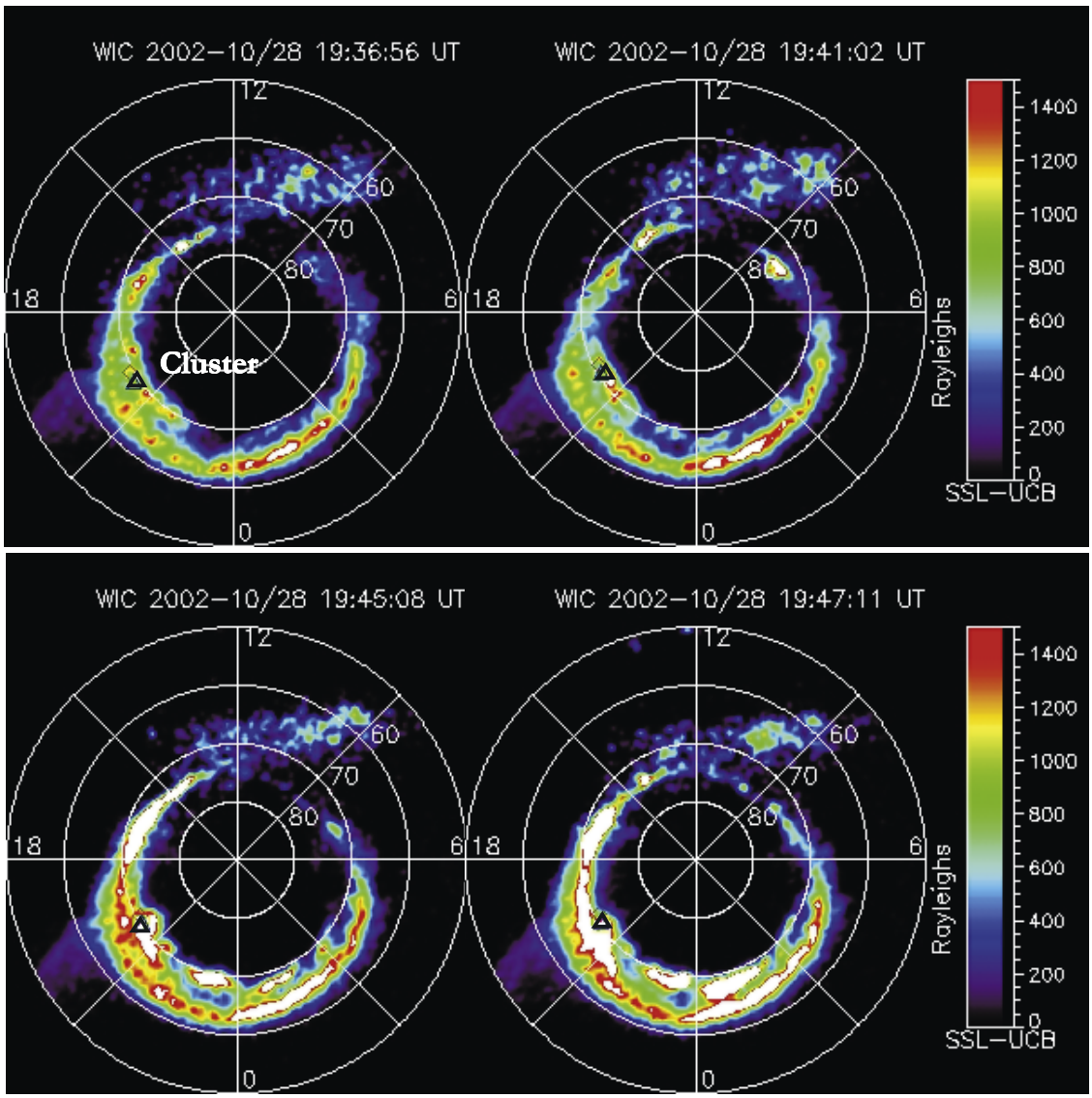

Figure 3. Selected IMAGE Wideband Imaging Camera (WIC) far ultraviolet images for the times shown on 28 October 2002. Images are projected onto the MLT-MLAT plane.

Hemisphere by Polar/UVI instrument (Figure 4). Note, the foot point of Cluster is not inside the Polar/UVI view; however, the time sequences of the auroral brightening and equatorward moving are consistent with IMAGE and Cluster observations. This intensification happened when Cluster observed the earthward moving plasmoid. The aurora shifted gradually to lower latitudes (60°) thereafter.

[17] The ionospheric effect of plasmoids is also recorded in the ground-based magnetometer data. The latitudinal distribution of westward currents in Figure 5 shows the results of the one-dimensional upward continuation of the ground magnetic perturbations [*Vanhamaki and Viljanen*, 2003], which allows one to reconstruct at each time step the density distribution of the east-west equivalent ionospheric currents crossing the meridian of the IMAGE magnetometer network (midnight at around 2130 UT) [*Viljanen and Hakkinen*, 1997]. The color code reflects the intensity of the westward equivalent current.

[18] It can be seen clearly that a westward equivalent current centered around 69^0 latitude moves gradually to lower latitude 67^0. The onset of the westward current starts at 1940 UT, and soon after the whole current moves equatorward. This feature is consistent with the earthward plasma flow and the moving plasmoid. It is interesting to note that the Cluster plasmoid activity observation coincides temporally as well as spatially with the excursion of the westward electrojet. As marked in the Figure 5, the onset times of the plasmoid and the inflection region of the first plasmoid can be clearly identified. The profile of the total current observed by Cluster (curlmeter) shown in Figure 2c is also consistent with the the westward electrojet. It should be mentioned here there is an area of small current densities at around 1946 UT. This region corresponds to the inflection point in the plasmoid. Moreover, the westward electrojet is clearly bifurcated into two areas at 68 deg and

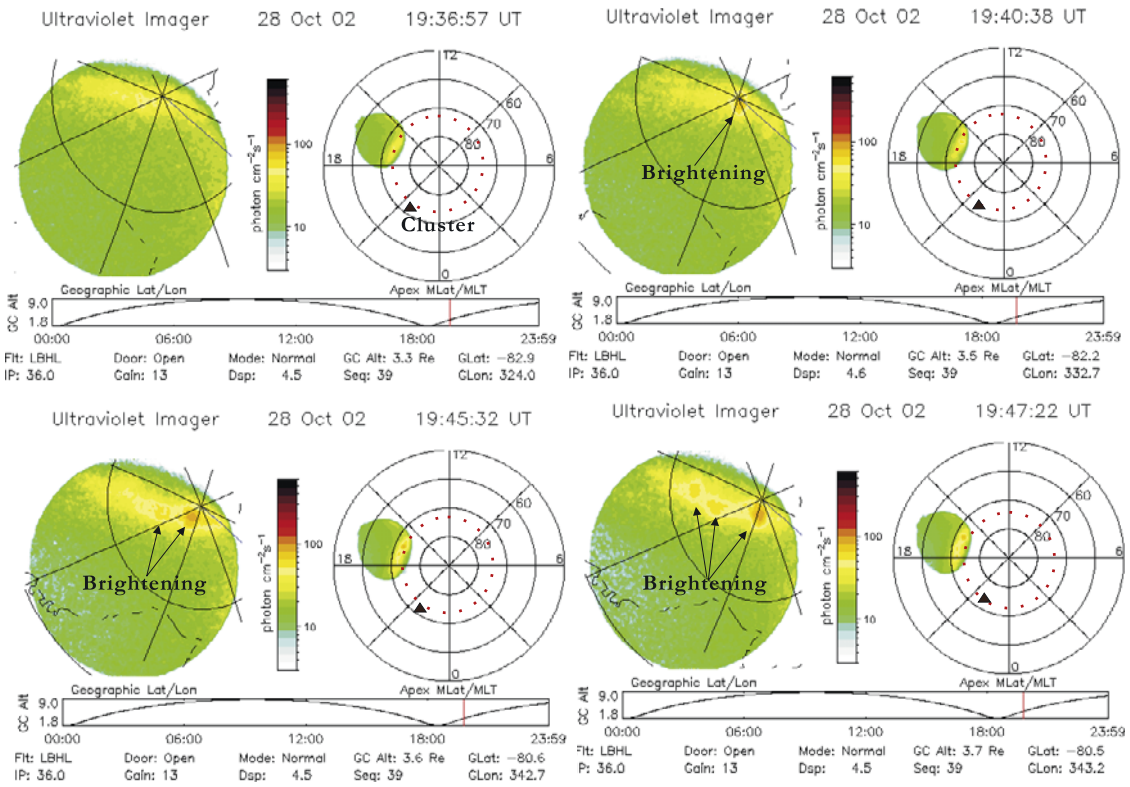

Figure 4. Selected Polar UVI images for the same time interval with Figure 3.

74 deg latitude. (This is also supported by MIRACLE all-sky cameras, not shown here.)

4. Discussion and Conclusion

[19] Figure 6 illustrates the relationship between the earthward moving plasmoid and the observed ionospheric signatures. Assuming that multiple reconnection occurs at the plasma sheet, a plasmoid is generated. It has been widely accepted that the bursty bulk flows (BBFs) will transport plasma flux and energy earthward and the energy will be further deposited in the Earth's ionosphere from the distant tail. In this paper we found that not only BBFs but also the magnetic structures, plasmoid and flux rope, will also play a significant role on such a flux and energy transport process. The ionospheric signatures observed in this paper are not substorm-related; the first injection in the geosynchronous orbit occurred at 2008 UT, 28 October 2002 which is about 44 min later than the ionospheric signature observed by ground-based IMAGE chain (Figure 5).

[20] The westward currents observed by the IMAGE magnetometer chain indeed demonstrated the plasmoid current closure through the substorm current wedge as shown in Figure 6. Owing to reduced plasma pressure inside the plasmoid (Figure 2), the cross-tail magnetic drift current inside the plasmoid is smaller than outside (Figure 2). The reduction of the current inside the plasmoid can be illustrated by adding a dusk to dawn current which close through the ionospheric electrojet analogy to the substorm current wedge, see Figure 6. The current sheet disturbances associated with the earthward moving plasmoid are indeed coincided with sudden enhancement of the westward equivalent current observed by the ground-based IMAGE chain (Figure 5). Since the current inside the plasmoid is smaller than outside and the earthward moving plasmoid is thus electrically polarized. Thus this plasmoid will charge up positive on the dawnside and negative on the duskside [*Chen and Wolf*, 1993; *Sergeev et al.*, 1996]. The polarization electric field inside plasmoid may be asymmetric because of the plasmoid significant Vy component toward the duskside. This leads to the observation by the Cluster spacecraft of unusually large bipolar electric fields E_x and E_y in the plasmoid.

[21] On the other hand, the flux rope core at around 1946 embedded in the earthward moving plasmoid may lead the interhemispheric current closure. The current inside the plasmoid indeed becomes more field-aligned (Figure 2b), although the magnitude turns to be smaller. This scenario is also supported by the following points:

[22] 1. As we can see in Figure 2, the energy for the most part of the plasmoid is dissipated ($\mathbf{J} \cdot \mathbf{E} < 0$); however, in the plasmoid core region the $\mathbf{J} \cdot \mathbf{E}$ is positive, indicating at this interval the plasmoid behaves as a "load," meaning that the electromagnetic energy is being loaded into in the plasmoid.

[23] 2. As shown in Figure 1b, the ionospheric origin singly charged oxygen ion V_x is tailward (this is different with proton V_x in Figure 1d). This is consistent with a field-aligned current coming from the Northern Hemisphere as shown in Figure 6.

[24] 3. The aurora in Southern Hemisphere is also observed UVI on board Polar satellite at around Lat. 75 degrees (http://uvisun.msfc.nasa.gov/DATA/).

[25] Further, the evolution of the westward currents observed by the ground-based IMAGE magnetometer chain and the aurora observed by the IMAGE satellite is also

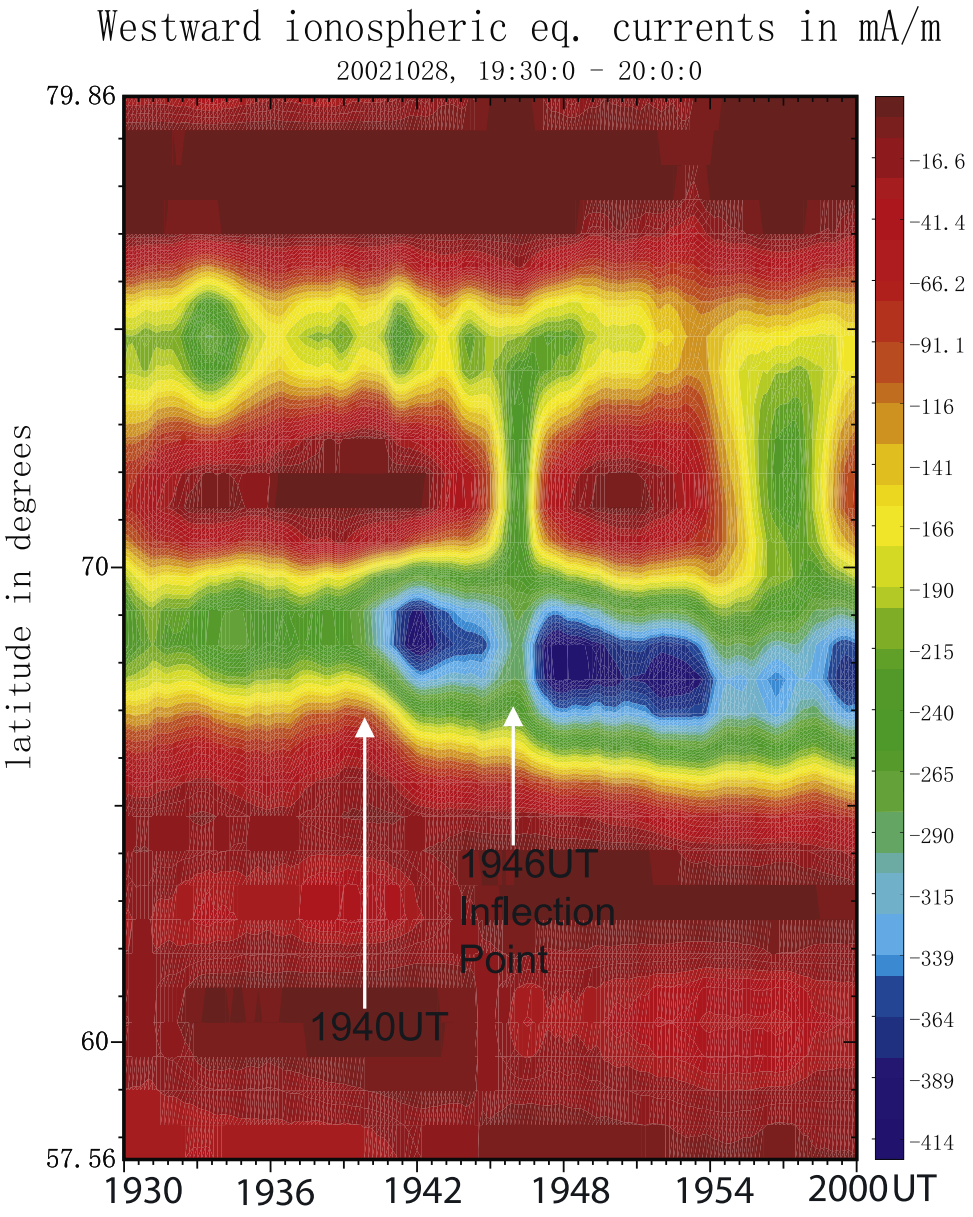

Figure 5. Latitudinal distribution of the westward currents near midnight reconstructed from data of the IMAGE magnetometer network using the one-dimensional upward continuation method [*Vanhamäki and Viljanen*, 2003].

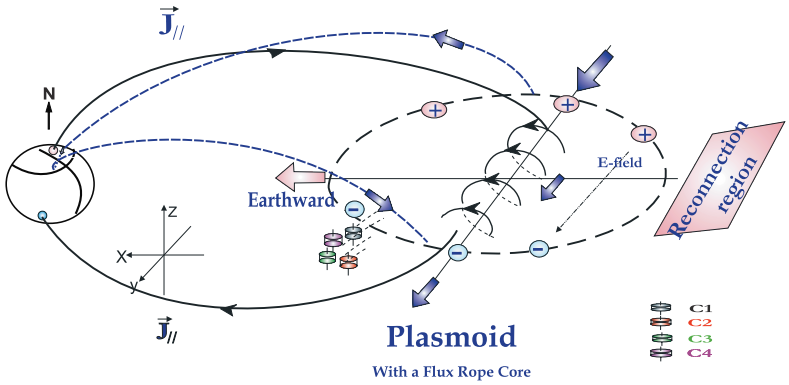

Figure 6. Illustration showing the relationship between the earthward moving plasmoid in the magnetosphere and ionospheric signature. The dashed line demonstrate substorm-like current wedge closure, whereas the solid line show an interhemispheric current closure.

consistent with the earthward motion of the plasmoid. The center of the original electrojet moved equatorward of the foot point indicating that part of the disturbance moved equatorward. The plasmoid therefore directly coupled with the ionospheric activity.

[26] **Acknowledgments.** This work is partly supported by NSFC projects 40528005 and 40374060 and by the CAS International Partnership Program for Creative Research Team.

[27] Zuyin Pu thanks X. H. Deng and Shinobu Machida for their assistance in evaluating this paper.

References

Baker, D. N., et al. (2002), Timing of magnetic reconnection initiation during a global magnetospheric substorm onset, *Geophys. Res. Lett.*, *29*(24), 2190, doi:10.1029/2002GL015539.

Balogh, A., et al. (1997), The cluster magnetic field investigation, *Space Sci. Rev.*, *79*, 65–91.

Chen, C. X., and R. A. Wolf (1993), Interpretation of high-speed flows in the plasma sheet, *J. Geophys. Res.*, *98*, 21,409–21,419.

Deng, X. H., H. Matsumoto, H. Kojima, T. Mukai, R. R. Anderson, W. Baumjohann, and R. Nakamura (2004), Geotail encounter with reconnection diffusion region in the Earth's magnetotail: Evidence of multiple X lines collisionless reconnection?, *J. Geophys. Res.*, *109*, A05206, doi:10.1029/2003JA010031.

Gustafsson, G., et al. (2001), First results of electric field and density observations by CLUSTER EFW based on initial months of operation, *Ann. Geophys.*, *19*, 1219–1240.

Hesse, M., J. Birn, M. Kuznetsova, and J. Dreher (1996), Simple model of core field generation during plasmoid evolution, *J. Geophys. Res.*, *101*, 10,797–10,804.

Ieda, A., S. Machida, T. Mukai, Y. Saito, T. Yamamoto, A. Nishida, T. Terasawa, and S. Kokubun (1998), Statistical analysis of the plasmoid evolution with Geotail observations, *J. Geophys. Res.*, *103*, 4453–4466.

Johnstone, A. D., et al. (1997), Peace: A plasma electron and current experiment, *Space Sci. Rev.*, *79*, 351–398.

Kivelson, M. G., K. K. Khurana, R. J. Walker, L. Kepko, and D. Xu (1996), Flux ropes, interheimspheric conjugacy, and magnetospheric current closure, *J. Geophys. Res.*, *101*, 27,341–27,350.

Nakamura, R., W. Baumjohann, R. Schoedel, M. Brittnacher, V. A. Sergeev, M. Kubyshkina, T. Mukai, and K. Liou (2001), Earthward flow bursts, auroral streamers and small expansions, *J. Geophys. Res.*, *106*, 10,719–10,802.

Paschmann, G., et al. (1979), Plasma acceleration at the Earth's magnetopause: Evidence for reconnection, *Nature*, *282*, 243–246.

Reme, H., et al. (1997), The cluster ion spectrometry (CIS) experiment, *Space Sci. Rev.*, *79*, 303–350.

Robert, P., M. W. Dunlop, A. Roux, and G. Chanteur (1998), Accuracy of current determination, in *Analysis Methods for Multi Spacecraft Data*, edited by G. Paschmann and P. W. Daly, p. 395, Eur. Space Agency, Bern, Switzerland.

Sergeev, V. A., V. Angelopoulos, J. T. Gosling, C. A. Cattell, and C. T. Russell (1996), Detection of localized, plasma-depleted flux tubes or bubbles in the midtail plasma sheet, *J. Geophys. Res.*, *101*, 10,817–10,826.

Slavin, J. A., et al. (2003a), Cluster electric current density measurements within a magnetic flux rope in the plasma sheet, *Geophys. Res. Lett.*, *30*(7), 1362, doi:10.1029/2002GL016411.

Slavin, J. A., et al. (2003b), Geotail observations of magnetic flux ropes in the plasma sheet, *J. Geophys. Res.*, *108*(A1), 1015, doi:10.1029/2002JA009557.

Vanhamäki, O. A. H., and A. Viljanen (2003), 1-dimensional upward continuation of the ground magnetic field disturbance using spherical elementary current systems, *Earth Planets Space*, *55*, 613.

Viljanen, A., and L. Häkkinen (1997), Image magnetometer network, in *Satellite-Ground Based Coordination Sourcebook, Magnetospheric Physics*, edited by M. W. M. Lockwood and H. Opgenoorth, *Eur. Space Agency Spec. Publ.*, *ESA-SP-1198*, 111–117.

Wilken, B., et al. (2001), First results from the rapid imaging energetic particle spectrometer on board cluster, *Ann. Geophys.*, *19*, 1355–1366.

Zong, Q.-G., et al. (1997), Geotail observation of energetic ion specics and magnetic field in plasmoid-like structures in the course of an isolated substorm event, *J. Geophys. Res.*, *102*, 11,409–11,428.

Zong, Q.-G., et al. (1998), Energetic oxygen ion bursts in distant magnetotail as a product of intense substorms: Three case studies, *J. Geophys. Res.*, *103*, 20,339–20,363.

Zong, Q.-G., et al. (2004), Cluster observations of earthward flowing plasmoid in the tail, *Geophys. Res. Lett.*, *31*, L18803, doi:10.1029/2004GL020692.

O. Amm, Geophysical Research Division, Finnish Meteorological Institute, Vuorikatu 15A, P. O. Box 503, F-00101 Helsinki, Finland.

D. N. Baker, Laboratory for Atmospheric and Space Physics, University of Colorado, 1234 Innovation Drive, Boulder, CO 80309-0590, USA.

J. B. Cao, State Key Laboratory for Space Weather, Chinese Academy of Sciences, 100080 Beijing, China.

P. W. Daly and A. Korth, Max-Planck-Institut für Sonnensystemforschung, Max Planck Str. 1, D-37189 Katlenburg-Lindau, Germany.

H. Frey, Space Science Laboratory, University of California, Berkeley, Grizzly Peak at Centennial Drive, Berkeley, CA 94720-7450, USA.

T. A. Fritz, Center For Space Physics, Boston University, 725 Commonwealth Avenue, Boston, MA 02215, USA.

S. Y. Fu, Department of Geophysics, Peking University, 100871 Beijing, China.

M. L. Goldstein and J. A. Slavin, NASA Goddard Space Flight Center, Code 612.2, Greenbelt, MD 20771, USA.

A. Pedersen, Department of Physics, University of Oslo, P. O. Box 1048 Blindern, N-0316 Oslo, Norway.

H. Reme, Centre d'Etude Spatiale des Rayonnements, 9, Avenue Colonel-Roche, B. P. 4346, F-31028 Toulouse, France.

P. Song and Q.-G. Zong, Center for Atmospheric Research, University of Massachusetts Lowell, 600 Suffolk Street, Lowell, MA 01854, USA. (quigang_zong@uml.edu)